

Chapter 38

The Structure Multivector

Michael Felsberg and Gerald Sommer

ABSTRACT The structure multivector is an operator for analysing the local structure of an image. It combines ideas from the structure tensor, steerable filters, and quadrature filters where the advantages of all three approaches are brought into a single method by means of geometric algebra. The proposed operator is efficient to implement and linear up to a final steering operation. In this paper we derive the structure multivector from the Laplace equation, which also introduces a new viewpoint on scale space. A phase approach for intrinsically 2D structures is derived and applications are presented which make use of the 2D part of the new operator.

38.1 Introduction and Motivation

In low level image processing, the main task is to extract the *structure* of an image. Most methods are somehow based on signal theory where the (gray scale) image is considered to be a real function on a 2D domain. The value of the function at a specific point indicates the intensity of light at that position. Unfortunately, the signal theory for 2D is poorly developed compared to 1D methods, since most approaches just project the 1D technique to 2D. In various cases, this procedure yields adequate or at least capable approaches like convolution, Fourier transform, and sampling. But there are also 1D techniques which are not applicable to images due to their *new quality* emerging from the higher dimension.

One of these 1D techniques is the *analytic signal* which extends a 1D real oscillation uniquely to a complex oscillation by means of the Hilbert transform. This extension enables us to decompose the 1D oscillation into its amplitude and phase information, which is especially useful for structure analysis of the signal.

While the modulus of the analytic signal represents the local energy of a signal, its local structure is represented by the argument. According to the Hermitian spectrum of a real signal, even and odd symmetry structures are represented by real and imaginary values, respectively. Forming any combination of both *symmetries*, we obtain a continuous 1D periodic space which is represented by the argument of the analytic signal: the local phase. The relation between the prototypical symmetries and the argument φ of the analytic signal is sketched in Figure 38.1.

Returning to images, the question is now: What is the appropriate 2D analytic signal? Since this question can be reduced to the 2D generalisation of

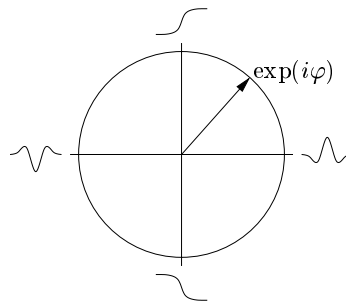


Figure 38.1. Relation between prototypical structures and the local phase φ . Adapted from [11].

the Hilbert transform, we will focus upon the latter. The generalised Hilbert transform was the motivation for developing the Calderón–Zygmund theory (for a nice survey of that topic of harmonic analysis see [20]) and indeed, our proposed solution can be understood as part of it. In this place, it should be mentioned that there exist several other attempts for a 2D Hilbert transform, which all have in common that they try to apply the 1D transform to the 2D signal. The best known is surely the partial Hilbert transform, where the spatial vector is projected onto a preference direction and the Hilbert transform of this scalar product is computed (see e.g., [11]). There are other approaches like the total Hilbert transform [12] or combinations of both (see also [4]). The common drawback is the missing isotropy of the transform, which means that the energy of the Hilbert transform is not invariant under rotations of the signal.

The just mentioned (missing) property reminds us of the principle of *invariance* and *equivariance* [11] or *split of identity*. These principles state that local properties should be *orthogonal*, i.e., that they are independent of each other. In the case of the analytic signal, the local amplitude only depends on the energy of the signal and the local phase only depends on the structure. Hence, the question rises: What should be the orthogonal properties of a 2D analytic signal? And further: How can we represent 2D structures? In order to give a first idea of the problems, we introduce the notion of the *intrinsic dimension* (see e.g., [15]) which can be identified with the degrees of freedom of a function. If an image is constant in a neighbourhood, its local intrinsic dimension is zero, if it is constant in one direction (edge, line), its local intrinsic dimension is one and in the remaining case it is two. In real images, local image structures are generally combinations of all these three cases. For intrinsically 0D (i0D) neighbourhoods, the 2D analytic signal should be zero (as for the 1D analytic signal) so no phase is needed. Structures which are i1D can be described by the local phase of the underlying 1D function. This phase should be *independen-*

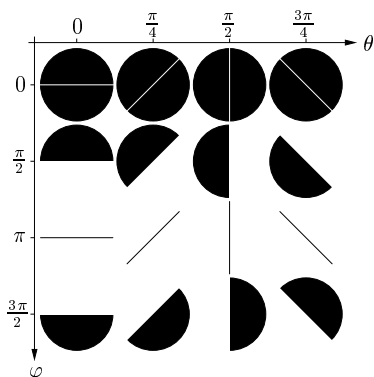


Figure 38.2. Intrinsically 1D signals (prototypes) with four orientations (θ) and four phases (φ).

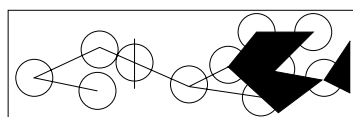


Figure 38.3. Different i2D signals (prototypes), some examples for i2D neighbourhoods are indicated by circles.

dent of the orientation¹ of the *i1D* structure. Accordingly, the orientation is introduced as an additional local property besides amplitude and phase, and all three properties are needed for a unique description of an *i1D* signal (see Figure 38.2).

Due to the fact that the classical phase has only one degree of freedom, it is *totally insufficient* for the description of *i2D* signals. Hence, for those signals a new phase approach with more degrees of freedom has to be derived, whereas it is totally unclear, how many degrees are necessary. The variety of *i2D* signals is striking, which is illustrated in Figure 38.3. In our new approach we try to decompose the *i2D* neighbourhood according to symmetry relations. Using this scheme, a 3D phase vector is sufficient.

Beside the partial Hilbert transform, we will relate our new approach to other capable methods, as there are the structure tensor / tensor of inertia [13] and steerable (quadrature) filters [1, 10]. The structure tensor fulfils the invariance – equivariance constraint for orientation and amplitude (i.e., it is isotropic, see [11]) but it includes no phase and is not linear since it is based either on the energy of quadrature filter responses or on products

¹In geometric algebra orientation is identified with the *sense of direction* of an object (e.g., oriented line). Conversely, in image processing, the orientation is defined modulo π and the orientation with sense (modulo 2π) is called ‘direction’.

of derivatives. The idea of steerable quadrature filters is to approximate the transfer function of the Hilbert transform (which is a rectangular in the angular coordinate) with spherical harmonics.

38.2 Mathematical Fundamentals

Signal processing in terms of linear shift-invariant operators is the engineering counterpart of harmonic analysis in mathematics. Harmonic analysis is closely related to harmonic functions, i.e., the solutions of the *Laplace equation*. Harmonic oscillations (short: harmonics) occur in the solutions of the wave equation. So do the harmonic functions which are solutions for the stationary case. Furthermore, harmonics can uniquely be extended to harmonic functions, which follows from the analytic extension of real functions on the line (1D case) and from the monogenic extension [3]².

In contrast to Clifford analysis, the starting point for all following derivations is the embedding of 2D signals in the 3D Euclidean space which is spanned by the orthonormal basis $\{\mathbf{e}_1, \mathbf{e}_2, \mathbf{e}_3\}$ (i.e., $\mathbf{e}_i \cdot \mathbf{e}_j = \delta_{ij}$). Therefore, 2D signals which are functions $\mathbb{R}^2 \rightarrow \mathbb{R}$ are ‘somehow’ extended to functions $\mathbb{R}^3 \rightarrow \mathbb{R}_{3,0}$.

For doing this extension, we apply the ideas of the papers [17] while translating them into engineers’ language. The fundamental equation we use is the Laplace equation

$$\Delta_3 \varphi(\mathbf{x} + s\mathbf{e}_3) = 0 \quad (38.1)$$

where Δ_3 is the Laplace operator of 3D space (i.e., $\Delta_3 = \partial_x^2 + \partial_y^2 + \partial_s^2$) and $\mathbf{x} = x\mathbf{e}_1 + y\mathbf{e}_2$. The reason for using s for the third coordinate instead of z and for keeping it distinct from \mathbf{x} will become obvious when we relate our approach to scale space ideas. The fundamental solution of the Laplace equation is the Newton potential $\varphi(\mathbf{x} + s\mathbf{e}_3) = |\mathbf{x} + s\mathbf{e}_3|^{-1}$, which means that any function convolved with the Newton potential is a solution of the 3D Laplace equation³. On the other hand, we can reformulate equation (38.1) as

$$\Delta_2 \varphi(\mathbf{x} + s\mathbf{e}_3) = -\partial_s^2 \varphi(\mathbf{x} + s\mathbf{e}_3) \quad (38.2)$$

where Δ_2 is the 2D Laplace operator. This equation can be solved by

²In higher dimensions, the uniqueness of the extension depends on the embedding space. In Clifford analysis, mainly two spaces are used: the space of paravectors or the $(n+1)$ D space [17]. In the latter case, the dimension of the algebra is doubled so that the uniqueness is only fulfilled in the even or odd grade subspace.

³In this context, ‘any function’ means every function that is interesting in real applications. For the formally correct formulation refer to mathematics literature, e.g., [5].

separation. With $\varphi(\mathbf{x} + s\mathbf{e}_3) = k(\mathbf{x})\hat{g}(s\mathbf{e}_3)$, the two PDEs

$$\Delta_2 k(\mathbf{x}) = -\omega^2 k(\mathbf{x}) \quad \text{and} \quad (38.3)$$

$$\partial_s^2 \hat{g}(s\mathbf{e}_3) = \omega^2 \hat{g}(s\mathbf{e}_3) \quad (38.4)$$

are obtained. The first one is solved by the (conjugated)⁴ Fourier kernel where ω is an angular frequency. Substituting $\omega^2 = 4\pi^2(u^2 + v^2) = 4\pi^2\mathbf{u}^2$ (so that $\mathbf{u} = u\mathbf{e}_1 + v\mathbf{e}_2$ is a 2D frequency vector) yields

$$k(\mathbf{x}) = \exp(\mathbf{e}_{12}2\pi \mathbf{x} \cdot \mathbf{u}) . \quad (38.5)$$

Since $\mathbf{e}_3^* = -\mathbf{e}_{12}$ in $\mathbb{R}_{3,0}$, the Fourier transform of a function $f(\mathbf{x})$ is embedded as

$$\hat{f}(\mathbf{x}) = \int_{\mathbb{R}^2} f(\mathbf{x}) \exp(\mathbf{e}_3^*2\pi \mathbf{x} \cdot \mathbf{u}) dx dy . \quad (38.6)$$

Note that this choice for the Fourier kernel is not the only possible solution. Any bivector B could replace \mathbf{e}_{12} since $\exp(B\alpha) = \cos \alpha + B \sin \alpha$ would yield the same transform, except for replacing i with B instead of \mathbf{e}_{12} . Furthermore, one could make use of complex Clifford algebras or negative signature spaces. It is also possible to introduce different base elements for both addends of the scalar product in (38.5) either in noncommutative or commutative hypercomplex algebras (see [4] resp. [6]).

Our choice was motivated by taking a simple algebra (neither complex nor negative signatures), by the affine theorem (which is not fulfilled in [4] and [6]), and by not preferring one of the base vectors of 2D space ($\pm\mathbf{e}_{12}$ is the only unit bivector so that its dual is orthogonal to both base vectors).

The second PDE (38.4) is solved by the *transfer function of a low pass filter*

$$\hat{g}(s\mathbf{e}_3) = \exp(-2\pi|\mathbf{u}|s) \quad (38.7)$$

if $s \in \mathbb{R}^+$. Behind this condition hide a lot of considerations of convergence and existence proofs which can be found e.g., in [17]. Actually, a formal mathematical treatment would be too technical in this context. Taking s in the open domain \mathbb{R}^+ is a practicable solution. The case when s tends to zero is called the *singular case* in the sequel.

The function $\varphi(\mathbf{x} + s\mathbf{e}_3) = k(\mathbf{x})\hat{g}(s\mathbf{e}_3)$ is now a solution of the original PDE (38.2). It looks similar to the kernel of the Laplace transform (e.g., [19]) which is natural because the Laplace kernel can be derived from the 2D Laplace equation. Since every linear combination of $\varphi(\mathbf{x} + s\mathbf{e}_3)$ for different vectors \mathbf{u} is also a solution of (38.2), we can also take the 2D integral over \mathbf{u} which is the inverse Fourier transform of $\hat{g}(\mathbf{u})$ (now considered as a function of \mathbf{u}). The low pass filter g is obtained using the Hankel transform table

⁴At this point, it is not obvious why we took the kernel of the inverse Fourier transform. The results further below will justify this choice.

in [2] to be

$$g(\mathbf{x} + s\mathbf{e}_3) = \frac{s}{2\pi|\mathbf{x} + s\mathbf{e}_3|^3} . \quad (38.8)$$

Since

$$\Delta_2 g(\mathbf{x} + s\mathbf{e}_3) = -\partial_s^2 g(\mathbf{x} + s\mathbf{e}_3) = \frac{3s(3\mathbf{x}^2 - 2s^2)}{2\pi|\mathbf{x} + s\mathbf{e}_3|^7} , \quad (38.9)$$

$g(\mathbf{x} + s\mathbf{e}_3)$ is shown to be a solution of the PDE (38.2). Note that $g(\mathbf{x} + s\mathbf{e}_3)$ is (up to a constant) the partial derivative of the Newton potential wrt. s :

$$\partial_s \frac{1}{|\mathbf{x} + s\mathbf{e}_3|} = -\frac{s}{|\mathbf{x} + s\mathbf{e}_3|^3} . \quad (38.10)$$

Therefore, we obtain the 3D generalisation of a well-known property of harmonic functions in 2D. The partial derivatives of a 2D harmonic function form a vector field which is irrotational and solenoidal (or as a complex function holomorphic). The components of such a vector field (holomorphic function) are again harmonic [14].

Comparing (38.8) to the fundamental solution of the heat equation (i.e., the Gaussian function [16]) shows several similarities:

- Both convolution kernels are *reproducing*, i.e., successive application is identical to a one-step application. They form a subalgebra of the convolution algebra.
- The PDEs for both problems are formally similar — the only difference is that (38.1) includes the second derivative wrt. s .
- The transfer functions of the fundamental solutions are the same up to the exponent of $|\mathbf{u}|$.
- Both approaches lead to a linear scale-space, i.e., an isotropic, linear multiscale interpretation.

While the Gaussian function has an uncertainty of $\frac{1}{2\pi}$, the new smoothing kernel has an uncertainty of $\sqrt{\frac{3}{2}} \frac{1}{2\pi}$, hence the location in phase space is slightly worse.

38.3 The Approach for i1D Symmetries

Nevertheless, we choose the new scale space since it is directly related to the *monogenic signal* which was introduced in detail in [8] embedded in the paravector space. In Euclidean vector space, it is obtained by the singular convolution operator

$$f_M(\mathbf{x}) = \lim_{s \rightarrow 0} \frac{\mathbf{x} + s\mathbf{e}_3}{2\pi(\mathbf{x}^2 + s^2)^{\frac{3}{2}}} * f(\mathbf{x}) \quad (38.11)$$

with the transfer function $(1 + \frac{\mathbf{u}^*}{|\mathbf{u}|})\mathbf{e}_3$. Taking the limit $s \rightarrow 0$, which is always done in the following, means that the original scale from the image formation is used. Eq. (38.11) also defines the Riesz transform with the kernel $h_1(\mathbf{x}) = \frac{\mathbf{x}}{2\pi|\mathbf{x}|^3}$. The monogenic signal of an image (scalar function) is a vector field $\mathbb{R}^2 \rightarrow \mathbb{R}^3$ which is obtained from $f(\mathbf{x})$ by the spinor field $a(\mathbf{x})$ according to $f_M = af\mathbf{e}_3$. Hence, $\frac{a}{|a|} = \frac{f_M\mathbf{e}_3}{|f_M|} = \exp(B\varphi)$ where $B(\mathbf{x})$ is a bivector field so that $B^* \cdot \mathbf{e}_3 = 0$ and B^* represents the *local orientation* in the signal (actually, B^* is orthogonal to the gradient of the signal, see also [7]) and we write $B^* = \cos\theta\mathbf{e}_1 + \sin\theta\mathbf{e}_2$. Furthermore, φ is the *local i1D phase*. For a more detailed discussion of the monogenic signal, orientation, and phase, see [7].

38.4 The Approach for i2D Symmetries

As mentioned in the introduction, we need an additional approach for symmetries which are intrinsically 2D. In order to design an appropriate method, we should consider three aspects of the previous section:

- The monogenic signal only consists of first derivatives of the Newton potential. We know from (differential) geometry that we need at least second-order derivatives for describing curvature, which is surely necessary for an i2D approach.
- The Calderón–Zygmund theory tells us that the Riesz transform is *not the only generalisation of the Hilbert transform*. The second-order derivatives of the inverse Laplace operator also generalise the Hilbert transform (see [20]).
- The components of (38.11) are obtained by transfer functions which are spherical harmonics of order zero and one. Higher spherical harmonics are related to higher derivatives in the spatial domain.

The second point constitutes the transfer function of the new operator to be a linear combination of $\{\frac{u^2}{\mathbf{u}^2}, \frac{v^2}{\mathbf{u}^2}, \frac{uv}{\mathbf{u}^2}\}$. From the third point and the identity $\exp(\mathbf{e}_{12}\alpha)^2 = \exp(\mathbf{e}_{12}2\alpha)$ it follows that the linear combination must be in $\{\frac{u^2-v^2}{\mathbf{u}^2}, \frac{2uv}{\mathbf{u}^2}\}$. Furthermore, we want to embed this second-order filter in the spinor part of a multivector (the vector part is given by the monogenic signal) and it is therefore natural to define the transfer function to be

$$\hat{h}_2(\mathbf{u}) = \frac{u^2 - v^2}{\mathbf{u}^2} + \frac{2uv}{\mathbf{u}^2}\mathbf{e}_{12} \quad (38.12)$$

and accordingly, the convolution operator reads

$$h_2(\mathbf{x}) = \frac{2(x^2 - y^2) - 4xy\mathbf{e}_{12}}{2\pi\mathbf{x}^4} \quad (38.13)$$

which can be proved using the Radon transform and the Residuum theorem.

For a combination of the monogenic signal and this new operator applied to f , we lose several properties of the first one, as there are possibilities for a combination with the new scale space approach and the relation to the theory of monogenic functions. We therefore calculate the monogenic signal of $h_2\mathbf{e}_3$ according to (38.11) where the basis vector \mathbf{e}_3 is introduced in order to stay in the spinor space. We obtain $h_3 + h_2$ where h_3 is given by the transfer function and the convolution kernel

$$\hat{h}_3(\mathbf{u}) = \frac{(3uv^2 - u^3)\mathbf{e}_{23} + (v^3 - 3u^2v)\mathbf{e}_{31}}{|\mathbf{u}|^3} \quad \text{and} \quad (38.14)$$

$$h_3(\mathbf{x}) = \frac{(3x^3 - 9xy^2)\mathbf{e}_{31} + (3y^3 - 9x^2y)\mathbf{e}_{23}}{2\pi|\mathbf{x}|^5}. \quad (38.15)$$

The convolution operator (38.15) is obtained by application of the symmetry relation of the Fourier transform to the Riesz transform and evaluation of the second derivatives. Since h_2 and h_3 use different base elements, we can combine them to a single spinor-valued function $h_2 + h_3 : \mathbb{R}^2 \rightarrow \mathbb{R}_{3,0}^+$.

38.5 The Structure Multivector

In order to suppress the energy at the main orientation (remember: we want to have an i2D operator, therefore, the i1D part of a signal must be suppressed), we have to set the transfer function to zero at the main orientation. At first, consider the orientation 0 where the transfer function reads $(\hat{h}_2 + \hat{h}_3)_{v=0} = 1 - \mathbf{e}_{23}$. Since we can only subtract transfer functions which are linear combinations of monogenic signals, we chose $1 + \frac{\mathbf{u}^*}{|\mathbf{u}|} = 1 + \hat{h}_1\mathbf{e}_3$. Therefore, $\hat{h}_2 - 1 + \hat{h}_3 - \hat{h}_1\mathbf{e}_3$ suppresses the energy at the orientation 0. Now consider an arbitrary main orientation θ_0 which is known from the monogenic signal. A rotation of the coordinate system by $-\theta_0$ reduces the general problem to the first case. This rotation is obtained by multiplying h_m with $\exp(\mathbf{e}_3^*m\theta_0)$ from the right: the operator is steered (this is possible because it is composed of spherical harmonics, see [1]). Hence, we define the i2D operator by

$$f_S = (h_3 * f) \exp \mathbf{e}_3^* 3\theta_0 + (h_2 * f) \exp \mathbf{e}_3^* 2\theta_0 - (h_1 * f \mathbf{e}_3) \exp \mathbf{e}_3^* \theta_0 - f \quad (38.16)$$

where f is a scalar signal.

Besides the suppression of the energy in the main orientation, the derived operator decomposes the spectrum according to its symmetries, which are similar to those of the quaternionic Fourier transform [4], see Figure 38.4, but they are not fixed to the coordinate system.

What is left for the i2D operator is the derivation of an appropriate phase approach. It is natural to identify the subalgebra of unit spinors with the group $\text{SO}(3)$. The resulting three Euler angles have specific semantics,

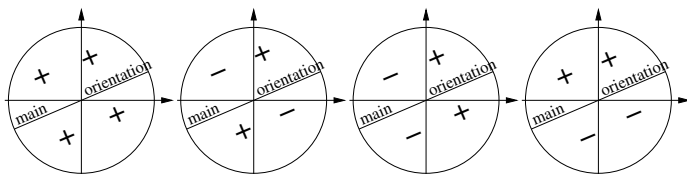


Figure 38.4. Symmetries of i2D operator from left to right: scalar part, e_{12} -part, e_{31} -part, and e_{23} -part.



Figure 38.5. Zero crossings of the impulse response of the i2D operator for different values of φ_2 (from left to right: 0, 0.57, 0.61, 0.79, 1.56).

which can be seen most easily by considering the impulse response (since the filter response is maximal for patterns which are most similar to the impulse response). The semantics of the three angles can be defined as follows: Two angles define the angle between the main orientation and the corner prototype and the corner prototype is given by the third phase. The three angles are obtained from the spinor decomposition

$$\frac{f_S}{|f_S|} = \exp(\mathbf{e}_{12}(\theta_2 - \theta_3)/2) \exp(\mathbf{e}_{31}\varphi_2) \exp(\mathbf{e}_{12}(\theta_2 + \theta_3)/2) \quad (38.17)$$

where φ_2 is related to the corner angle, θ_2 is proportional to the angle between the main orientation and the corner-prototype with angle $\pi/2$, and θ_3 is proportional to the angle between main orientation and the corner-prototype with angle $\pi/3$. Therefore, f_S is a *generic model* for all kinds of simple junctions, where simple junction means that two edges or lines forming the junction can have arbitrary angles. Y-junctions are only included, if two edges or lines of the ‘Y’ have the same orientation, or the ‘Y’ is symmetric. In Figure 38.5, the zero crossings of the impulse responses for some different values of φ_2 are presented, which shows that all corner angles can be modelled. Finally, the combination of monogenic signal and the i2D operator response forms the *structure multivector* $f_{SM} = f_M + f_S$, an entity which includes information about local amplitude, local phase, and local geometry (main orientation and relative orientations θ_2 and θ_3) of both, the i1D parts and the i2D parts of a 2D signal.

38.6 Conclusion

A straightforward application of the i2D operator is corner detection/classification and curvature estimation. We have applied the i2D operator to

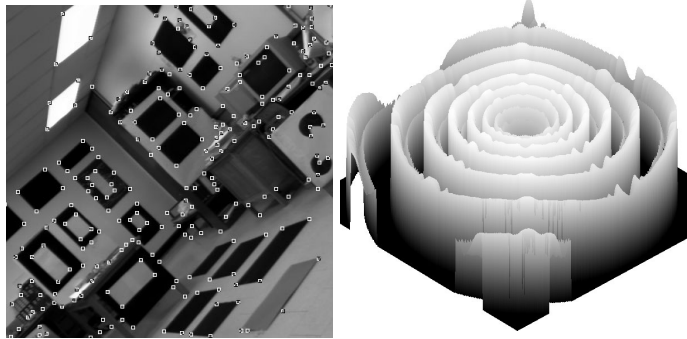


Figure 38.6. Left: Filter response of the i2D operator applied to the lab-image. Right: Amplitude of filter output for a logarithmic spiral. The amplitude is multiplied with the radius to show the linear dependency.

five images from the web⁵ and thresholded the energy of the filter response. The results are similar to those of the css-approach [18], the result for the lab-image can be found in Figure 38.6 on the left. The result can be compared to those of the Kitchen/Rosenfeld detector, the Susan detector, the Plessey detector, and the css-approach by visiting the mentioned webpage. Our method is based on the energy of the operator only, but an improvement by taking the i2D phase into account is possible. Also the classification has not been implemented yet.

In order to investigate the behaviour of the i2D operator for different curvatures, we applied it to an image of a logarithmic spiral (product of curvature and radius is constant). The resulting amplitude of the filter output is visualised in Figure 38.6 on the right, which shows that the amplitude is linearly increasing with the curvature. Applications of the monogenic signal can be found in [9].

Finally, we have shown that the structure multivector is an advanced method for the description of local properties of a 2D signal. In contrast to the structure tensor, which only takes the local energy into account, we have introduced phase approaches for both, i1D and i2D neighbourhoods. Beside the i2D phase, the main difference wrt. classical quadrature filters is the isotropy of our method. For the representation of i1D structures, the structure multivector is a linear approach in contrast to steerable quadrature filters. The i2D part of our method only includes a *minimal nonlinearity*, which means that only the final steering is a nonlinear operation. As a consequence, our method yields a low computational load because it consists of only seven real (scalar) convolutions and two subsequent spinor multiplications and additions.

⁵URL: <http://www.ee.surrey.ac.uk/Research/VSSP/demos/corners>

Acknowledgements

This work has been supported by German National Merit Foundation and by DFG Graduiertenkolleg No. 357 (M. Felsberg) and by DFG Grant So-320-2-2 (G. Sommer).

References

- [1] Andersson, M. T., Controllable Multidimensional Filters and Models in Low Level Computer Vision, Ph.D. thesis, Linköping Univ., Sept. 1992.
- [2] Bracewell, R. N., *Two-Dimensional Imaging*, Prentice Hall Signal Processing Series. Prentice Hall, Englewood Cliffs, 1995.
- [3] Brackx, F., Delanghe, R., and Sommen, F., *Clifford Analysis*. Pitman, Boston, 1982.
- [4] Bülow, T., Hypercomplex Spectral Signal Representations for the Processing and Analysis of Images, Ph.D. thesis, Christian-Albrechts-University of Kiel, 1999.
- [5] Burg, K., Haf, H., and Wille, F., *Höhere Mathematik für Ingenieure, Band V Funktionalanalysis und Partielle Differentialgleichungen*, Teubner Stuttgart, 1993.
- [6] Felsberg, M., Bülow, T., and Sommer, G., Commutative hypercomplex Fourier transforms of multidimensional signals. In *Geometric Computing with Clifford Algebras* (G. Sommer, ed.), Springer-Verlag, Heidelberg, 2001. To be published.
- [7] Felsberg, M., and Sommer, G., The monogenic signal, Tech. Rep. 2009, Institute of Computer Science and Applied Mathematics, Christian-Albrechts-University of Kiel, Germany, September 2000.
- [8] Felsberg, M., and Sommer, G., The multidimensional isotropic generalization of quadrature filters in geometric algebra. In *Proc. Int. Workshop on Algebraic Frames for the Perception-Action Cycle, Kiel* (G. Sommer and Y. Zeevi, eds.), vol. 1888 of *Lecture Notes in Computer Science*, Springer-Verlag, Heidelberg, 2000, pp. 175–185.
- [9] Felsberg, M., and Sommer, G., A new extension of linear signal processing for estimating local properties and detecting features, In *22. DAGM Symposium Mustererkennung, Kiel* (G. Sommer, ed.), Springer-Verlag, Heidelberg, 2000, pp. 195–202.



- [10] Freeman, W. T., and Adelson, E. H., The design and use of steerable filters, *IEEE Trans. PAMI* **13** **9** (1991), 891–906.
- [11] Granlund, G. H., and Knutsson, H., *Signal Processing for Computer Vision*, Kluwer Ac. Publ., Dordrecht, 1995.
- [12] Hahn, S. L., *Hilbert Transforms in Signal Processing*, Artech House, Boston, London, 1996.
- [13] Jähne, B., *Digitale Bildverarbeitung*, Springer-Verlag, Berlin, 1997.
- [14] Krantz, S. G., *Handbook of Complex Variables*, Birkhäuser, Boston, 1999.
- [15] Krieger, G., and Zetsche, C., Nonlinear image operators for the evaluation of local intrinsic dimensionality, *IEEE Transactions on Image Processing* **5**, 6 (June 1996), 1026–1041.
- [16] Lindeberg, T., *Scale-Space Theory in Computer Vision*, The Kluwer Int. Series in Eng. and Comp. Sci., Kluwer Ac. Publ., Boston, 1994.
- [17] McIntosh, A., Clifford algebras, Fourier theory, singular integrals, and harmonic functions on Lipschitz domains. In *Clifford Algebras in Analysis and Related Topics* (J. Ryan, ed.), Studies in Advanced Mathematics. CRC Press, Boca Raton, 1996, pp. 33–88.
- [18] Mokhtarian, F., and Suomela, R., Robust image corner detection through curvature scale space, *IEEE Trans. Pattern Anal. Machine Intell.* **20**, 12 (1998), 1376–1381.
- [19] Schiff, J. L., *The Laplace Transform*, Undergraduate Texts in Mathematics, Springer-Verlag, New York, 1999.
- [20] Stein, E. M., Singular integrals: The roles of Calderón and Zygmund, *Notices of the American Mathematical Society* **45**, 9 (1998), 1130–1140.